Magnetic palm kernel biochar potential route for phenol removal from wastewater

Muhammad Nazmi Hairuddin[1] · Nabisab Mujawar Mubarak[1] · Mohammad Khalid[2] · Ezzat Chan Abdullah[3] ·
Rashmi Walvekar[4] · Rama Rao Karri[5]

Abstract

The pollution of water resources due to the disposal of industrial wastes that have organic material like phenol is causing worldwide concern because of their toxicity towards aquatic life, human beings and the environment. Phenol causes nervous system damage, renal kidney disease, mental retardation, cancer and anaemia. In this study, magnetic palm kernel biochar is used for removal of phenol from wastewater. The effect of parameters such as pH, agitation speed, contact time and magnetic biochar dosage are validated using design of experiments. The statistical analysis reveals that the optimum conditions for the highest removal (93.39%) of phenol are obtained at pH of 8, magnetic biochar dosage of 0.6 g, agitation speed at 180 rpm and time of 60 min with the initial concentration of 10 mg/L. The maximum adsorption capacities of phenol were found to be 10.84 mg/g and Langmuir and Freundlich isotherm models match the experimental data very well and adsorption kinetic obeys a pseudo-second order. Hence, magnetic palm kernel can be a potential candidate for phenol removal from wastewater.

Keywords Palm kernel · Magnetic biochar · Wastewater · Isotherm · Adsorption · Phenol

Introduction

Nowadays, water quality is deteorating due to large number of pollutants which needs great priority due to concern from Malaysia is getting polluted and needs priority concern from the authorities and local government. One of the factors of the water pollution occurrence is the rapid growth in the manufacturing industry and the beginning of usage of synthetic chemicals major sources since the early twentieth century (Owa 2013). Generally, the sources of water pollution are from agriculture, sewer system, commercial, domestic waste and industrial waste (Molva 2004). The industrial process produces a lot of products and by-products which have severe risks and health issues to human beings such as carcinogenic, mutagenic and toxicity properties (Elwakeel et al. 2018; Elwakeel et al. 2015; Pradeep et al. 2015). In addition, the industrial wastewater from the manufacturing halogenated organics release a very high concentration of the hazardous compound, and the amount of concentration may reach as high as hundreds of mg/L (Pradeep et al. 2015). There are also

✉ Nabisab Mujawar Mubarak
mubarak.yaseen@gmail.com

✉ Mohammad Khalid
khalids@sunway.edu.my

✉ Ezzat Chan Abdullah
ezzatchan@gmail.com; ezzatc@utm.my

Rama Rao Karri
karri.rao@utb.edu.bn

[1] Department of Chemical Engineering, Faculty of Engineering and Science, Curtin University, 98009 Miri, Sarawak, Malaysia

[2] Graphene & Advanced 2D Materials Research Group (GAMRG), School of Science and Technology, Sunway University, No. 5, Jalan Universiti, Bandar Sunway, 47500 Subang Jaya, Selangor, Malaysia

[3] Department of Chemical Process Engineering, Malaysia-Japan International Institute of Technology (MJIIT), Universiti Teknologi Malaysia (UTM), Jalan Sultan Yahya Petra (Jalan Semarak), 54100 Kuala Lumpur, Malaysia

[4] Sustainable Energy and Green Technology Research Group (SEGT), School of Engineering, Taylor's University, 47500 Subang Jaya, Selangor, Malaysia

[5] Petroleum and Chemical Engineering, Faculty of Engineering, Universiti Teknologi Brunei, Mukim Gadong A, Brunei Darussalam

many other types of industrial wastes that have organic material which has difficulties to be removed using conventional biological treatment processes (Farhod 2010). Wastewater refers to all discharge liquid waste or sewage from the domestic and commercial areas (Amoatey and Bani 2011). The sources of wastewater are from the mixture of agriculture, sewer, commercial, domestic and industrial activities (Gami et al. 2014). Globally, approximately two million tons of wastewater from industrial, sewage and agricultural waste are produced in the world every day (Taylor 2003). There is also approximately 1500 km^3 amount of wastewater produced annually, which is six times more than the amount of water in all existing rivers in the world (Taylor 2003). Major industries are widely using certain chemicals and organic materials to produce their desired product. Each process of production in the industry could produce different hazardous waste due to the long steps taken, which involve a lot of reactions (Pradeep et al. 2015). To consider waste as a hazardous substance, it must be reactive, corrosive, ignitable and toxic (Sihem et al. 2012). Based on a study made by Molva ,2014, there is around 95% of the chemical that has been acknowledged as hazardous and toxic chemical by referring to its amount of production, exposure and living side effects (Molva 2004). One of the top listed chemicals which is classified as the toxic and hazardous chemical is phenolic compound. Phenol is usually used as a raw material in the industry to produce a lot of chemical products such as petrochemicals, pesticides, dyes, pharmaceuticals and plastics (Abdelwahab and Amin 2013).

Phenolic compounds have a high concentration of toxic and can be absorbed directly into the human body. United States Environmental Protection Agency (USEPA) (Bohdziewicz et al. 2012) and European Union (Chakraborty et al.) clarified that phenol is one of the pollutions that must be under priority concern due to its toxicity (Jiboury 2013). In a study, phenol has been classified by USEPA to be the 11th out of 126 chemicals as a priority pollutant due to their level of toxicity (Farhod 2010). Another government environmental agencies like World Health Organization (WHO) (Panagos et al. 2013) (Hsieh et al. 2008), European Council Directive (Tziotzios et al. 2005), Japan Ordinance Law No. 15 (Dahalan 2014), United Arab Emirates (UAE) (Al Zarooni and Elshorbagy 2006), Department of Environment (DOE) in Malaysia (Gupta and Ahmad 2012) and Argentina based on Law 24051 have provided certain regulation of phenol concentration before releasing it to the environment (Coniglio et al. 2008).

Therefore, elimination of phenol is a necessity to protect the environment and human beings (Abdelwahab and Amin 2013). The technology of phenol removal and treating the wastewater is growing extensively (Karri et al. 2017a). But every technology has its own disadvantage in terms of infrastructure and efficiency of the removal process. Therefore, magnetic biochar is invented for phenol removal and other types of hazardous wastes in the wastewater. Magnetic biochar is a new magnetic carbon adsorbent which is produced from different types of biomass that shows the good magnetic property (Mubarak et al. 2016). There are three different methods of synthesis of magnetic biochar, which are pyrolysis method, co-precipitation method and calcination method (Thines et al. 2017b). Recently, many studies showed that usage of magnetic biochar for environmental application for removal of heavy metals and dyes from wastewater (Chakraborty et al. 2005; Elgarahy et al. 2019; Qiu et al. 2009). The example types of biomass that have been used as magnetic biochar are corn cob (Ma et al. 2015), cereal by-product (Sihem et al. 2012), paper mill sludge (Devi and Saroha 2014), sawdust (Dakhil 2013), olive mill waste (Abdelkreem 2013) and palm kernel shell (Karri et al. 2017a; Karri and Sahu 2018; Karri et al. 2017b; Mubarak et al. 2016). The materials can be found widely as agricultural waste, and they contain a high amount of mineral and high porosity size (Thines et al. 2017b). The size of porosity could affect the adsorption rate of the organic material. Therefore, the higher the porosity size of the magnetic biochar, the higher the adsorption rate (Ayotte et al. 2001). The usage of magnetic biochar would not jeopardize the environment as the source of it is from agricultural material waste. One of the advantages of using magnetic biochar is can be simply removed from the soil matrix whenever the necessity ascends using simple principles of magnetism synthesised palm.

In this research study, a palm kernel magnetic biochar is used to test the adsorption capacity for phenol removal from wastewater together with the single factor optimization and statistical optimization of the process parameters like pH, agitation speed, contact time and magnetic biochar dosage. The study of isotherm and kinetic model are investigated. The thermodynamic study for phenol removal and characterization of magnetic biochar were also investigated in this research.

Materials and methods

Materials

The source of the palm kernel magnetic biochar production is similar to previous research work (Thines et al. 2017a). Meanwhile, the source of the phenol crystal is purchased from Sigma-Aldrich Malaysia with assistance from the Curtin laboratory staff.

Purification of palm kernel magnetic biochar

The palm kernel magnetic biochar sample is taken from the supervisor, and it is left soaked for 1 day. Then, the magnetic biochar is filtered with distilled water until it reaches its neutral pH value. Then, it was dried in a Memmert oven at 80 °C for 24 h. Once the sample becoming dry, it is stored in a bottle which is closed tightly. The purpose of purification is to

dehydrate the palm kernel magnetic biochar until it can achieve constant weight.

Preparation of stock solution and reagents

The stock solution of phenol was prepared by diluting the phenol crystal with the mass of 0.01 g into 1 L of distilled water to produce phenol solution of 10 mg/L which is set to become initial concentration and used in the batch adsorption studies. One hundred millilitres of 0.1 M of hydrochloric acid (HCl) and 100 mL of 0.1 M of sodium hydroxide (NaOH) solution were prepared to diverge the pH of phenol solution from pH 4, pH 6 and pH 8.

Batch adsorption studies

A series of experiment has been done by having a consistent value of the initial concentration of phenol solutions of 10 mg/L. The process parameters like agitation speed, pH value, agitation time and adsorbent dosage, as shown in Table 1, are varied to find the optimum condition for the adsorbent to give the maximum adsorption capacity. For each set of experiment, it has been done using 100 mL of 10 mg/L of phenol solution and the experiment is carried out using 100 mL of the conical flask at the room temperature. The mixing of the phenol solution and the adsorbent is being done using the KS-501 IKA WERKE Orbital Shaker with a different set of process parameters.

After the mixing process, the phenol solutions are filtered using Whatman filter paper with a diameter of 125 mm. The filtered phenol solutions are placed into closed tight tube; meanwhile, the adsorbents are transferred in zip lock bags for further tests. The absorbance of filtered phenol solution is measured by using Perkin Elmer UV-VIS Spectrophotometer at a wavelength of 270 nm together with a standard phenol solution and distilled water. The result of the final concentration of the phenol solution is gained from the final absorbance values, and the concentration is calculated using Beer's Law at the end of all the test. Then, the percentage of removal of phenol and the adsorption capacity is calculated using Eqs. 1 and 2 shown below:

$$\text{Percentage Removal of Phenol} = \frac{C_i - C_f}{C_i} \times 100 \quad (1)$$

Table 1 Parameters used in batch adsorption studies

Process parameters	Range of values
pH of phenol solution	pH 4, pH 6, pH 8
Contact time	10 min, 30 min, 50 min
Agitation speed	80 rpm, 130 rpm, 180 rpm
Adsorbent dosage	0.20 g, 0.40 g, 0.60 g

$$\text{Adsorption Capacity} \ (q_t) = \frac{[(C_i - C_f) \ V]}{M} \quad (2)$$

Where q_t is adsorption capacity (mg/g) at time t, C_i is phenol solution initial concentration (mg/L), C_f is phenol solution final concentration (mg/L), M is palm kernel magnetic biochar weight (g) and V is volume of the phenol solution (L).

Modelling of adsorption isotherm and kinetic study

The adsorption isotherm and kinetic study for removal of phenol is investigated by having phenol solutions at different concentrations (10 mg/L, 20 mg/L, 30 mg/L, 40 mg/L, 50 mg/L, 60 mg/L, 70 mg/L) and constant parameters like magnetic biochar dosage 0.6 g, maximum contact time of 100 min, agitation speed of 180 rpm and pH of phenol solution of pH 8. The samples are taken at a certain time interval and are filtered using filter paper. The final concentrations of the samples are analysed to determine the residual amount of phenol left in the aqueous solutions.

The inherent adsorption mechanisms can be identified by fitting the equilibrium experimental data to the conventional isotherms. Table 2 summarizes several isotherm models which expressed in non-linear forms. Most of the researchers use the linear form, for simplicity of evaluating the isotherm parameters by fitting the data to the conventional kinetic models. In this study, two conventional kinetic models, which are pseudo-First and Second order, and two intraparticle diffusion models, namely Boyd and Weber–Morris, kinetic models, were investigated. The respective expressions that describe the kinetic models are presented in Table 3, respectively.

Characterization of palm kernel magnetic biochar

For the physical structure and morphology of palm kernel magnetic biochar before and after adsorption are tested using field emission scanning electron microscope (FESEM). For the effect of the surface functional group of the palm kernel, magnetic biochar is tested using the Fourier transform infrared

Table 2 Various forms of isotherm models for single component expressed non-linear forms

Type of isotherm	Non-linear expression
Freundlich	$q_e = K_F C_e^{1/n_F}$
Langmuir	$q_e = \left(\frac{q_m K_L C_e}{1 + K_L C_e} \right)$
Redlich–Peterson	$q_e = \left(\frac{K_R C_e}{1 + a_R C_e^{n_R}} \right)$
Sips	$q_e = \left(\frac{K_S b_s C_e^{n_s}}{1 + b_s C_e^{n_s}} \right)$

Table 3 Summary of different conventional types of kinetics used to estimate the adsorption rate

Type of kinetics	Non-linear form
Pseudo-1st order	$q = q_e\left(1 - e^{-k_1 t}\right)$
Pseudo-2nd order	$q = \left(\frac{K_2 q_e^2}{1 + tK_2 q_e}\right)t$
Weber–Morris model	$q = k_{id}\sqrt{t}$
Boyd model	$\frac{q}{q_e} = 1 - \frac{6}{\pi^2}\exp(-Bt);\ Bt = -0.4977 - \ln(1 - F)$ for $F\ (= q/q_e) > 0.85;\ B = \frac{\pi^2 D_i}{r^2}$

spectrophotometer (FTIR). Lakeshore-7300 vibrating sample magnetometer (VSM), the saturation magnetization of palm kernel magnetic biochar, is tested to see magnetic field and magnetization of the adsorbents.

Results and discussion

Effect of dosage

A series of experiments has been made to identify the optimum condition for the dosage of magnetic biochar needed to be used for the removal of phenol. The amount of dosage of magnetic biochar being used in these experiments are 0.2 g, 0.4 g and 0.6 g. The result is calculated from the initial concentration of phenol solution and the final concentration of phenol solution after being removed by magnetic biochar at a certain amount of the dosage. The expected outcome of this experiment is that the percentage of removal of phenol increases as the number of magnetic biochar increases. From the graph in Fig. 1, it is shown that the highest percentage occurs at a dosage of 0.6 g of removal of phenol which is 90.7% occurs at the highest amount of dosage, which is 0.6 g. The reason is that the higher the amount of dosage used in the reaction, the higher the number of the active site
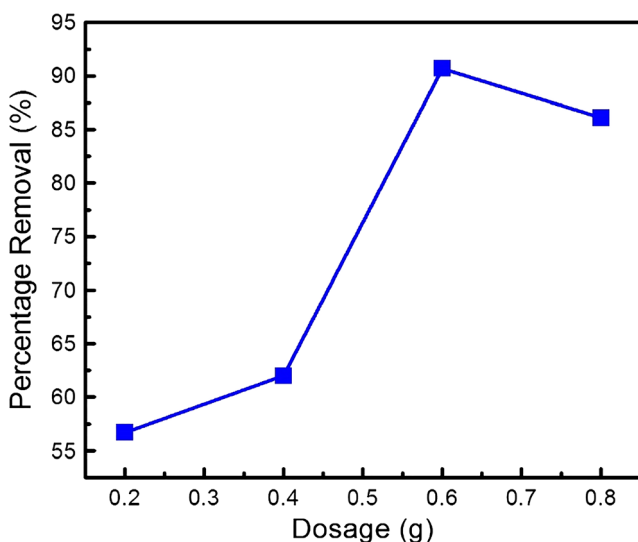
available for phenol to adsorb to the surface of palm kernel magnetic biochar (Gao et al. 2017) (Shahamat et al. 2014). Once the active side of the magnetic biochar is fully occupied, the desorption process occurs, which can be seen at a dosage amount of 0.8 g by carrying out a set of experiment.

Effect of agitation speed

The experiment is also being done by varying the speed of the orbital shaker once the magnetic biochar intact with phenol solution, which are 80 rpm, 130 rpm and 180 rpm. The results are calculated from the initial concentration of phenol solution and phenol concentration after being removed by magnetic biochar at a certain speed. The expected result of the experiment is that the removal percentage of the phenol will increase as the speed of the orbital shaker increases. From the graph in Fig. 2, it is shown that the highest percentage of removal of phenol which is 90.7% occurs when the speed of the shaker is at 180 rpm. It is because the higher speed of the orbital shaker affects the rate of diffusion of phenol molecules that become higher when it is surrounding the magnetic biochar particle due to the high speed and reducing the liquid boundary layer thickness (Asmaly et al. 2015) (Archana et al. 2016) (Kargari and Abbassian 2015). Once the rate of diffusion of phenol molecule at optimum speed has achieved, a set of experiment has been carried out to identify desorption process has occurred which can be seen at the orbital shaker speed at 200 rpm.

Effect of contact time

The effect of contact time for removal of phenol is shown in Fig. 3. A series of experiments are also being carried out by varying the amount of time contact of phenol solution and magnetic biochar, which are 10 min, 30 min and 50 min. The result is calculated from the initial concentration of
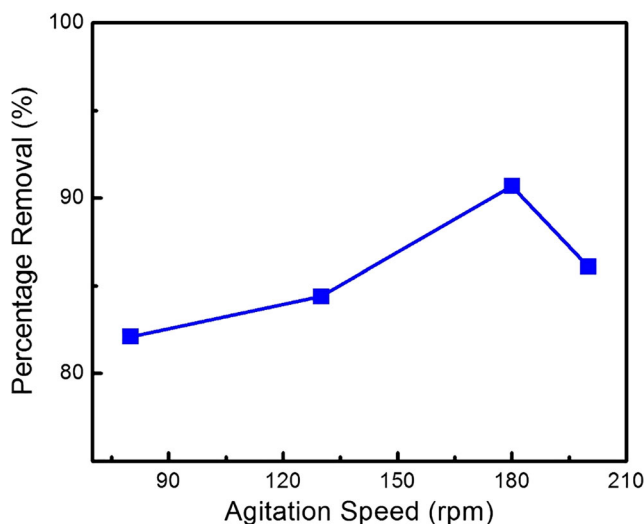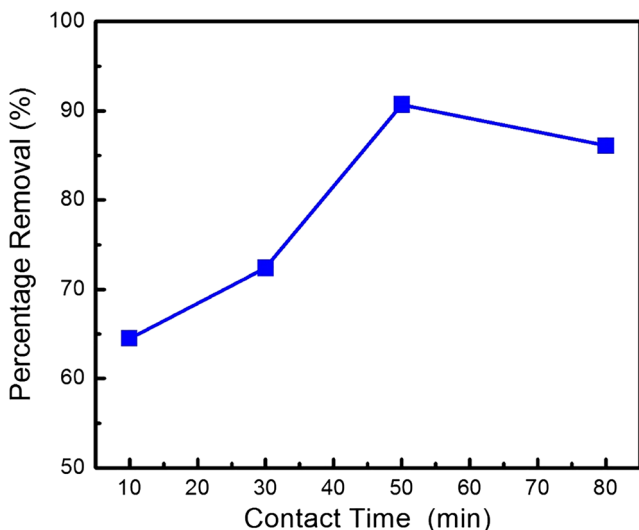

Fig. 1 Effect of dosage

Fig. 2 Effect of agitation speed

Fig. 3 Effect of contact time

Fig. 4 Effect of pH

phenol solution and the final concentration of phenol being removed by magnetic biochar by the certain duration of contact time. The expected result of the experiment would be as the contact time of the phenol solution, and magnetic biochar increase, the removal percentage of phenol will increase. Figure 3 shows that the highest percentage of removal of phenol which is 90.7% occurs when the contact time is at 50 min. This is because as the contact time increases, phenol compound and magnetic biochar have a longer time to interact between each other (Gholizadeh et al. 2013) (Abdel-Ghani et al. 2014) (Dilekoglu 2016). A set of experiment has been carried out to identify the desorption process of phenol solution occurrence, which then occurs at the contact time of phenol solution and palm kernel magnetic biochar reach 80 min.

Effect of pH for removing phenol

The experiment has also been done by changing the value of pH of the phenol solution, which is from 4 to 9. The results are calculated from the initial concentration of phenol solution based on their pH values and the final concentration of phenol being removed by magnetic biochar at certain pH values. The expected result of this experiment is that as the value of pH of phenol solution increased, the removal percentage of phenol will increase. From the graph in Fig. 4, it is shown that the highest percentage of removal of phenol which is 90.7% occurs when the pH values are at pH 8. The reason for the effect of the pH of the phenol solution is because of the surface properties of the palm kernel magnetic biochar compared to the other types of carbon adsorbents and the concentration difference of $[OH^-]$ and $[H^+]$ in the phenol solution (Yap et al. 2017) (Alam et al. 2009b) (Said et al. 2013). The palm kernel magnetic biochar has a positive active side, which could reduce its adsorption capacity when it is under a low pH solution setting (Alam et al. 2009a) (Zhang et al. 2017). A
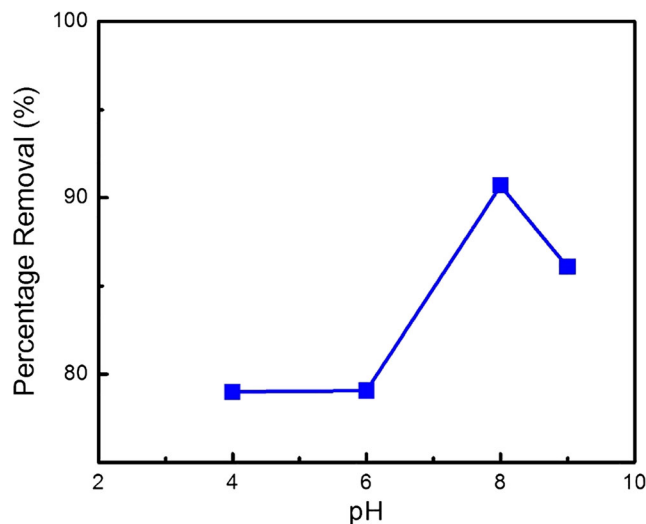
set of experiment has been carried out to show the desorption process for phenol removal occurred after it has achieved its optimum condition, which is pH 9.

Statistical analysis for removal of phenol

The statistical analysis for the percentage of removal of phenol is being done using Design-Expert software. The number of runs needed is generated by the design of experiment (DOE) by referring to the process parameters inserted, as shown in Table 1. The study is needed to determine the highest percentage of removal of phenol and the most optimum condition for the removal of phenol. The analysis of the removal of phenol is continued by carrying out "analysis of variance" (ANOVA) as shown in Table 4.

From the result generated by the ANOVA application in Table 4, the result of fisher F-test is 17.40; it shows that the model is significant. Fisher F-test shows the evaluation of the mean square of the residuals (errors). The value of F is high, which shows that the model is highly efficient; meanwhile, the low p value shows that the regression model is highly significant. The lack of fit shows insignificant result from the error occurs during the experiment does not affect the efficiency of the model. The model equation that progressed for the phenol removal in aqueous solution by using palm kernel magnetic biochar is shown in Eq. 3 as follows:

$$\text{Percentage of Removal of Phenol } (\%) \tag{3}$$
$$= 90.50 - 7.42\,A + 10.49\,B + 10.62\,C$$
$$+ 10.70\,D - 0.38\,AB$$
$$+ 4.82\,AC - 0.81\,AD - 1.97\,BC - 1.29\,BD - 1.34$$
$$CD - 12.24\,A^2 - 4.19\,B^2 - 8.84\,C^2 - 5.34\,D^2$$

Table 4 ANOVA for removal of phenol

Source	Sum of squares	df	Mean square	F-value	p value	Status
Model	15,691.98	14	1120.86	17.40	< 0.0001	Significant
A-pH	1321.65	1	1321.65	20.52	0.0004	
B-dosage	2936.70	1	2639.70	40.99	< 0.0001	
C-speed	2707.25	1	2707.25	42.04	< 0.0001	
D-time	2749.90	1	2749.90	42.70	< 0.0001	
AB	2.33	1	2.33	0.0361	0.8518	
AC	371.53	1	371.53	5.77	0.0297	
AD	10.40	1	10.40	0.1615	0.6935	
BC	62.02	1	62.02	0.9629	0.3420	
BD	26.78	1	26.78	0.4158	0.5288	
CD	28.89	1	28.89	0.4486	0.5132	
A^2	4109.70	1	4109.70	63.81	< 0.0001	
B^2	481.68	1	481.68	7.48	0.0153	
C^2	2143.73	1	2143.73	33.29	< 0.0001	
D^2	782.33	1	782.33	12.15	0.0033	
Residual	966.04	15	64.40			
Lack of fit	966.04	10	96.60			Insignificant
Pure error	0.0000	5	0.0000			
Cor total	16,658.03	29				

Subsequently, the variable generated A, B, C, D, AB, AC, AD, BC, BD, CD, A^2, B^2, C^2, D^2 are important terms model. Where A is the pH values, B is the amount of dosage of magnetic biochar, C is the agitation speed of the orbital shaker and D is the contact time. Based on Eq. 3, the negative signs indicate antagonistic effect values; meanwhile, the positive signs indicate synergistic effect values. Figure 5 shows the 3-D plot of interaction of process parameters for removal of phenol.

From the observation of the 3-D interaction plot for the dosage of magnetic biochar against time, the highest percentage of removal is obtained at the end, which is 60 min and 0.8 g of dosage, respectively. It is because of the higher number the dosage of magnetic biochar used in the reaction, the number of active site concentration available for phenol to adsorb to the surface of magnetic biochar which leads to an adjustment of the electrostatic charge and removal of the H^+ ions. Meanwhile, the pH of phenol solution affects the adsorption rate and the percentage of removal of phenol in the aqueous solution as observe to the 3-D plot interaction between pH against speed due to the surface properties of the palm kernel magnetic biochar compared to the other types of carbon adsorbents and the concentration difference of $[OH^-]$ and $[H^+]$ in the phenol solution. For the 3-D interaction plot of contact time against the agitation speed of the shaker, the highest percentage of removal of phenol occurs at the middle point, which is 60 min and 200 rpm. The longer the contact time between the phenol solution with the magnetic biochar which makes it have a longer time to interact with each other and allow more adsorption to occur to the active site of the magnetic biochar.

Characterization of palm kernel magnetic biochar using FESEM analysis

FESEM, field emission scanning electron microscopy, is the equipment used to perceive the physical surface morphology, which is palm kernel magnetic biochar. The FESEM model used in this research is FEI Quanta 400. FESEM is used to observe the structure of the raw or pure palm kernel magnetic biochar and the after phenol adsorption of magnetic biochar at the magnification scale of 500 nm and 10 μm (Yap et al. 2017; Mubarak et al. 2016; Anyika et al. 2017). Figure 6 a and b show the FESEM image of palm kernel magnetic biochar before phenol adsorption and Fig. 6c, d shows the FESEM image of palm kernel magnetic biochar after phenol adsorption. Nitrogen gas is used as diffusion oxidizing agent for the carbonaceous matrix as it also assists in the removal of the carbon consumption and impurities which leads to porosity widening during the chemical activation (Mubarak et al. 2016). The opening of the microporosity on the biochar surface leads to larger pores formation, and the porous structure is widened for FESEM images result at different magnification scale (Ruthiraan et al. 2017, 2019).

Characterization of palm kernel magnetic biochar using FTIR analysis

The effect of the surface functional group of the palm kernel magnetic biochar is tested using the Fourier transform infrared spectrophotometer (FTIR) using a Perkin Elmer model. The equipment is to identify the adsorption of phenol in the

Fig. 5 3-D plot of phenol removal using magnetic palm kernel. **a** Interaction of dosage and time. **b** Interaction of agitation speed and pH. **c** Interaction of agitation speed and time

magnetic biochar by observing the chemical reactivity of the surface of magnetic biochar and porosity of the magnetic biochar (Mubarak et al. 2016). The chemical reactivity of the surface could be seen specifically in the arrangement of chemisorbed oxygen by different functional groups (Anyika et al. 2017). The result of the graph is to see the difference between the wavenumber and transmittance percentage of the non-adsorbed magnetic biochar and adsorbed magnetic

Fig. 6 **a**, **b** Before adsorption of FESEM. **c**, **d** After adsorption of phenol

biochar. Figure 7 a shows the result of the surface functional group and transmittance value at certain wave number for palm kernel magnetic biochar without any adsorption of phenol component. Meanwhile, Fig. 7b shows the result of the surface functional group and transmittance value at the certain wave number for palm kernel magnetic biochar after adsorption of phenol components.

From the graph of FTIR images above, it shows that the functional group of pure magnetic biochar and magnetic biochar after phenol adsorption can be impregnated on the surface of palm kernel magnetic biochar. From Fig. 7a, the band of the plots for pure magnetic biochar located at 3746.2 cm^{-1} and 3610.2 cm^{-1} is related to single bond stretch component, C-H. The band which located at 2153 cm^{-1} and 2024.7 cm^{-1} is related to triple bond components (alkynes), $C \equiv C$. Then, the band which is located at 1737 cm^{-1} and 1700.3 cm^{-1} is related to double bond components (ketone or aldehyde), C=O. Meanwhile, the band located at wavenumber 1543.3 cm^{-1} is related to double bond component (alkene), C=C. Lastly, the predicted function group at wave number 562.2 cm^{-1} would be C-H.

From the FTIR image after phenol adsorption shown in Fig. 7b, the band located at wave number 3746.2 cm^{-1} has the single bond stretch component, C-H and the band located at wave number 3728 cm^{-1} also has the single bond stretch component which is O-H. Next, the band located at wave number 2919.5 cm^{-1} and 2851.5 cm^{-1} has the single stretch bond components (carboxylic acid), O-H. Next, the band located at wave number 2155.5 cm^{-1} has a triple bond component (alkyne), $C \equiv C$. Next, the band located at wave number 1543.3 cm^{-1} has a double bond component (alkene), C=C. Lastly, the predicted functional group using FTIR image at wave number 695.62 cm^{-1} and 559.6 cm^{-1} would be C-O components. Based on the comparison with the previous researches, the result of this FTIR images shows good arrangement as predicted.
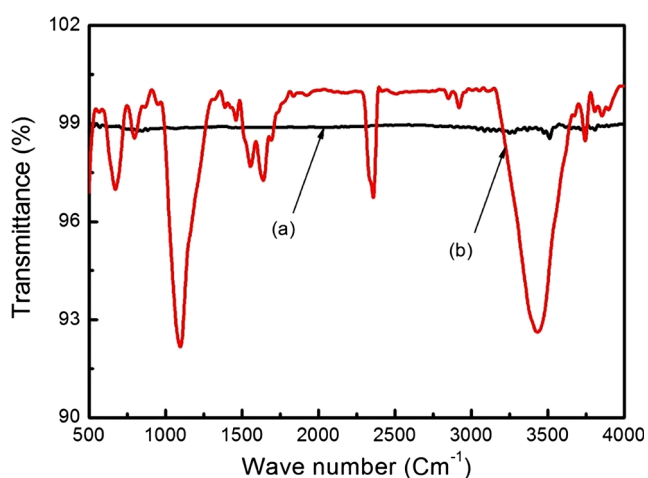
Characterization of palm kernel magnetic biochar from saturation magnetization

The magnetic properties of palm kernel magnetic biochar are carried out from the measurement of coercivity (Gauss) and saturation magnetization (emu/g) at room temperature (Mubarak et al. 2016). The result is recorded in the graph of magnetization (emu/g) against the magnetic field (A. et al.) which is shown in Fig. 8. The curve slope of the graph shows the magnetic properties of pure palm kernel magnetic biochar and palm kernel magnetic biochar after phenol adsorption. From the curve, the magnetization of the palm kernel magnetic biochar after phenol adsorption is slightly higher compared to the pure one is due to the presence of additional superparamagnetic constituents (Baig et al. 2016) which is also affected from size of grain, density of both magnetic biochar, A-B exchange contact and anisotropy (Lee et al. 2001; Mubarak et al. 2016; Zhang et al. 2013). The smaller value of magnetization (emu/g) for pure palm kernel magnetic biochar is due to the presence of non-magnetic carbon, weak magnetic properties and small particle size compared to the after phenol adsorption's magnetic biochar (Wu et al. 2015). The increasing magnetization value leads to increasing crystallinity structure (Tao et al. 2008). From the previous researches, the materials that have superparamagnetic behaviour should be widely applied for treating the environment especially for the removal of chemical contaminants (Xin et al. 2016) (Zhang et al. 2013).

Adsorption isotherm study for removal of phenol

To interpret the phenol adsorption onto the magnetic biochar, the most appropriate isotherm model has to be identified. In this regard, the conventional isotherm models summarized in Table 2 were investigated. Generally, as reported in many recent
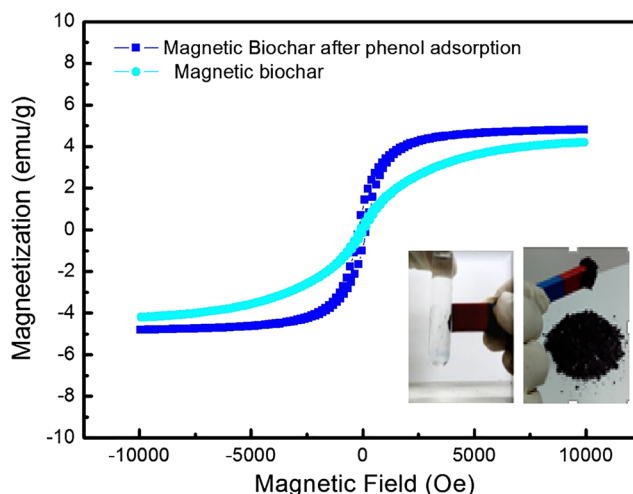

Fig. 7 a FTIR adsorption spectra for **a** magnetic palm kernel biochar before and **b** magnetic palm kernel biochar after phenol adsorption

Fig. 8 Saturation magnetization of magnetic palm kernel biochar and magnetic palm kernel biochar after phenol adsorption
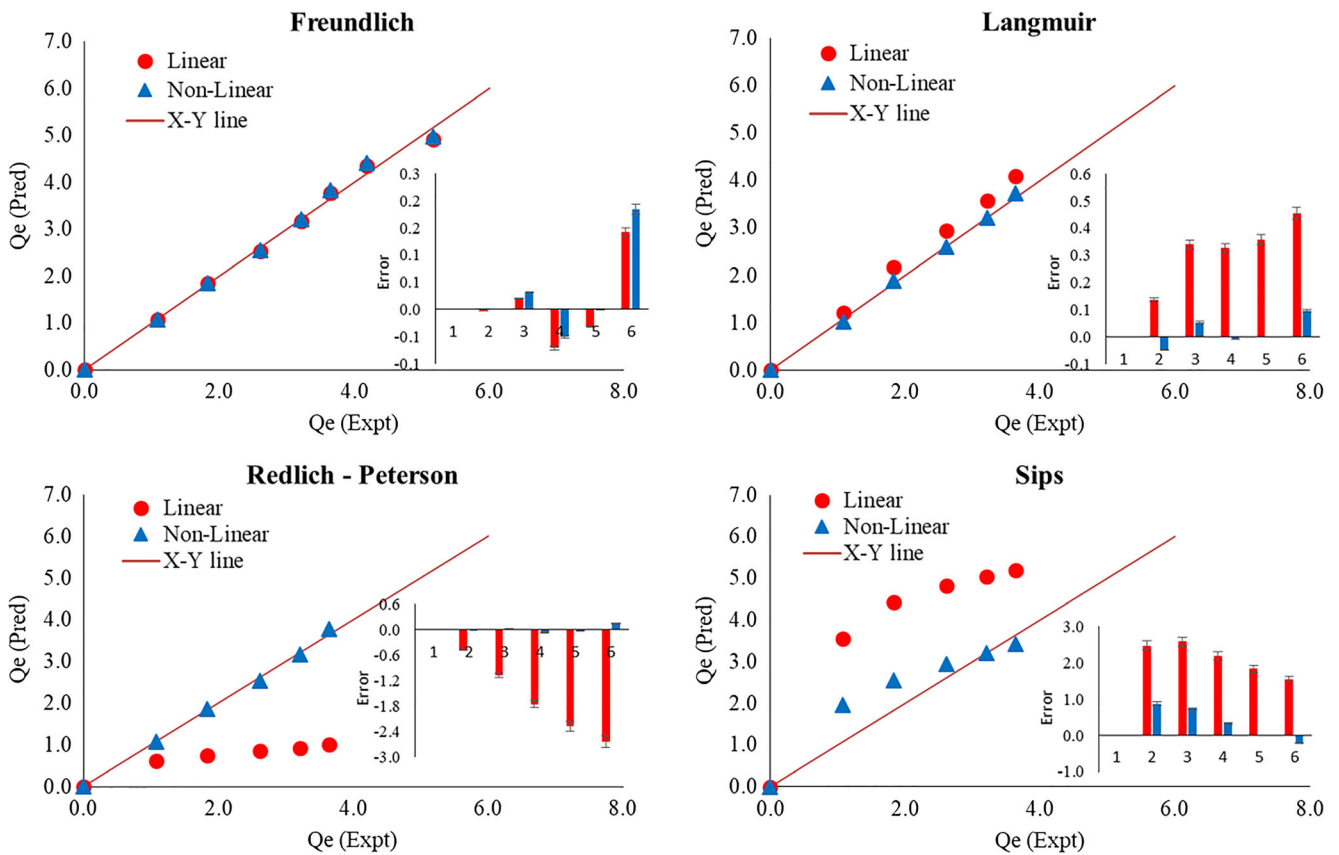
Fig. 9 Comparison of linear and non-linear isotherms against the measured values

studies (Alam Khan and Ahmad 2016; Inyinbor et al. 2016; Rincón-Silva et al. 2016), the parameters of the isotherm models are obtained by linearizing the corresponding non-linear expression, and the parameters are determined by fitting a regression line. However, due to this linearization procedure, the

characteristics of non-linear isotherm models are meddled, and sensitivity is misinterpreted (Tran et al. 2017). Therefore, to uphold the non-linear nature, the model (non-linear) parameters need to be estimated with an appropriate technique (Karri et al. 2017b; Karri et al. 2018; Lingamdinne et al. 2018).

Fig. 10 Performance of different isotherms depicting the phenol adsorption onto biochar
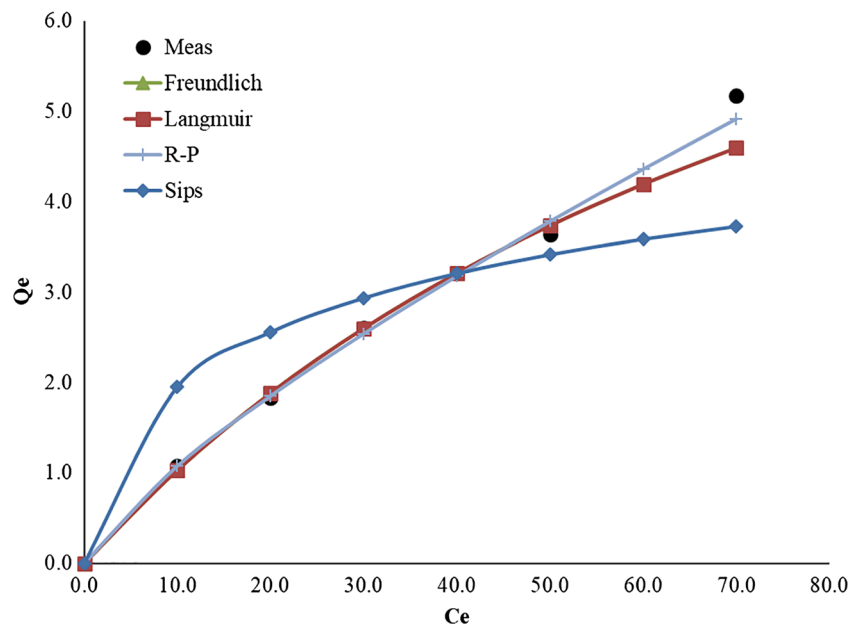
Table 5 Statistical metrics of four isotherm models when evaluated both linear and non-linear approach

Isotherms →	Langmuir		Freundlich		Redlich–Peterson		Sips	
	Linear	Non-linear	Linear	Non-linear	Linear	Non-linear	Linear	Non-linear
Para (1)	$q_m = 10.02$	10.84	$K_F = 0.18$	0.18	$K_R = 96.32$	118.67	$K_S = 5.94$	6.14
Para (2)	$K_L = 0.01$	0.01	$1/n_F = 0.78$	0.79	$a_R = 322.18$	662.98	$n_S = 1.05$	1.62
Para (3)					$n_R = 0.69$	0.22	$b_s = 0.17$	0.11
R^2	0.97	0.98	0.99	0.99	0.97	0.99	0.85	0.94
ARE	16.07	4.33	3.58	3.54	93.43	3.58	117.09	36.26
SAE	2.21	0.79	0.69	0.68	15.43	0.69	11.97	4.20
RMSE	0.43	0.29	0.17	0.18	3.28	0.17	2.49	0.99
HYBRID	8.61	2.33	0.91	0.99	370.24	0.91	440.46	51.14
MPSD	29.33	15.26	9.54	9.95	192.42	9.54	209.87	71.51

To identify the inherent mechanisms of phenol adsorption onto the magnetic biochar, the experimental data is validated with four conventional isotherms namely, Freundlich, Langmuir, Redlich–Peterson and Sips isotherms. Figure 9 depicts the performance of each isotherm model, when evaluated by both linear and non-linear approaches. It can be observed that the experimental data perfectly follow Langmuir isotherm model, which has resulted with R^2 of 0.97 and 0.98 for both linear and non-linear approaches, respectively. Hence, the model predicted values lie on the x-y line. It is also observed that the non-linear Langmuir model predictions also have high correlation with experimental values. It is also observed that the phenol adsorption process follows Freundlich isotherm model which resulted in R^2 of 0.99. Since the adsorption process follows both Langmuir and Freundlich isotherm models, so the experimental data is further validated on the typical hybrid isotherm (Redlich–Peterson) model. This isotherm model has three isotherm constants (K_R, a_R and α) and hence called 3-parameter isotherm model. The performance of all the identified four isotherms that depicts the phenol adsorption onto biochar is shown in Fig. 10. The quality of performance presented in this figure establishes that the phenol adsorption process using magnetic palm kernel biochar follows the Freundlich and Langmuir isotherm models.

To further confirm these observations, the non-linear statistical metrics which quantifies the magnitudes of the errors and provides a scale for quantifying good measure of accuracy is evaluated for all the model predicted results. The non-linear statistical metrics evaluated here are average relative error (ARE), sum of absolute error (SAE), root means square error (RMSE), hybrid fractional error (HYBRID) and Marquardt's percentage std dev (MPSD). These metrics are shown in Table 5, for all the four isotherm models. All the statistical values thus resulted are within the acceptable limits and better for non-linear expressions. Since the RMSE is lower and R^2 is higher for Freundlich isotherm model, so phenol adsorption process using magnetic palm kernel biochar follows this isotherm model. The maximum adsorption capacity (q_m) is 10.02 mg/g, which shows that adsorption is likely to occur in room temperature.

Adsorption kinetic studies for removal of phenol

Kinetic modelling is an approach to estimate the sorption rate as well as to find best suitable adsorption rate expressions that represent possible mechanisms. In general, the overall rate of adsorption is assumed to be due to the adsorption rate of the solute on the surface of the adsorbent and due to intraparticle diffusion. The mechanism of adsorption process be influenced

Table 6 Statistical metrics of four kinetic models when evaluated both linear and non-linear approach for concentration of 10 mg/L

| Kinetics →	Pseudo-first order		Pseudo-second order		Weber and Morris		Boyd plot	
	Linear	Non-linear	Linear	Non-linear	Linear	Non-linear	Linear	Non-linear
Para (1)	$k_1 = 0.0434$	0.0276	$k_2 = 0.0033$	0.0033	$k_{id} = 0.113$	0.141	$B = 0.063$	0.024
Para (2)	$q_e = 1.2100$	1.2100	$q_e = 3.1770$	3.1781			$q_e = 1.210$	1.210
R^2	0.975	0.983	0.983	0.992	0.979	0.983	0.943	0.964
SAE	15.472	7.416	0.503	0.502	15.961	4.849	56.736	10.817
RMSE	0.106	0.119	0.008	0.008	0.191	0.060	0.364	0.122
HYBRID	15.929	11.694	0.958	0.955	19.555	8.031	73.074	17.824
MPSD	0.972	0.976	1.000	1.000	0.929	0.971	0.800	0.905
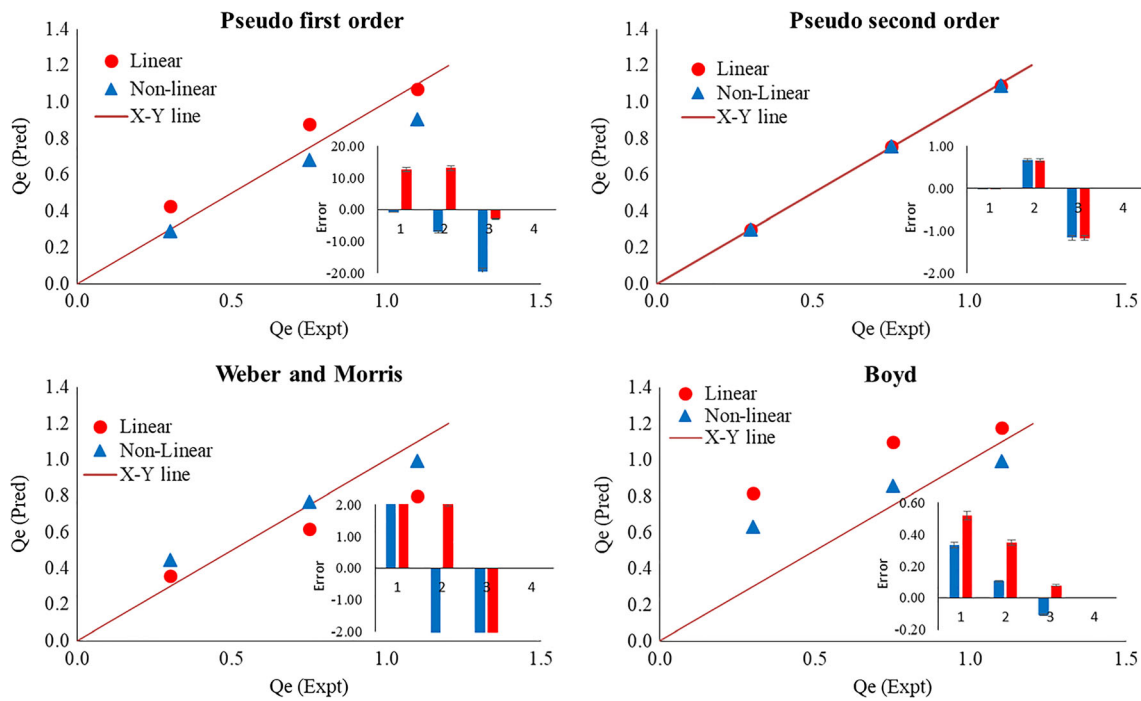
Fig. 11 Comparison of linear and non-linear kinetic model predictions against the measured values for concentration of 10 mg/L

by the chemical and/or physical characteristics of the adsorbent. Several forms of kinetic models have been proposed in literature to describe the adsorption mechanism. In this research study, the conventional kinetic models (pseudo-first order, second order) and intraparticle diffusion models namely Weber–Morris and Boyd are investigated. The non-linear expressions of the above four kinetic models are given in Table 6. In this study, the kinetic modelling study was conducted at different concentrations (10 mg/L, 20 mg/L, 30 mg/L, 40 mg/L, 50 mg/L, 60 mg/L and 70 mg/L). All these experiments are carried at a constant values like magnetic biochar dosage of 0.6 g, maximum contact time of 100 min, agitation speed of 180 rpm and pH of 8.

To investigate the adsorption rate, the kinetic modelling is done for each concentration. The identified four kinetic

models are fitted to the experimental data as shown in Fig. 11. The results presented in this figure are for concentration of 10 mg/L. It can be observed the traditional fitting of linearized kinetic model using least square methods results in inferior model predictions. The non-linear model predictions for all the kinetic models are very appreciable and significant. It can be observed that the pseudo-second-order model perfectly depicts the kinetics of phenol adsorption.

To further confirm these observations, the non-linear statistical metrics which quantifies the magnitudes of the errors and provides a scale for quantifying good measure of accuracy is

Table 7 Pseudo-first-order model and pseudo-second-order model kinetic parameters

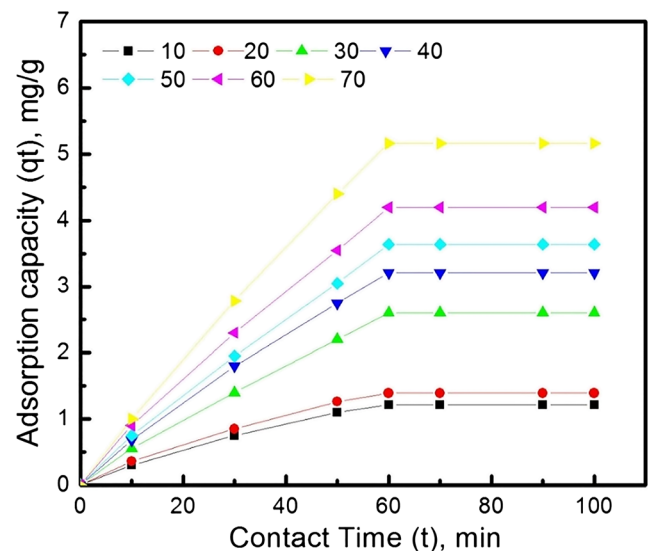|	Pseudo-first order		Pseudo-second order		
Concentration	K_1	R^2	q_e	K_2	R^2
10 mg/L	0.0276	0.982	3.1781	0.0033	0.992
20 mg/L	0.0246	0.874	3.4959	0.0029	0.883
30 mg/L	0.0229	0.815	5.4028	0.0027	0.823
40 mg/L	0.0204	0.727	6.0384	0.0024	0.734
50 mg/L	0.0188	0.668	7.6274	0.0022	0.675
60 mg/L	0.0155	0.550	8.8987	0.0018	0.556
70 mg/L	0.0135	0.481	10.1699	0.0016	0.486

Fig. 12 Adsorption capacity (q_t) versus contact time (t) with different initial phenol solution concentration in mg/L

Table 8 Thermodynamic study for phenol adsorption

Concentration C_o (mg L^{-1})	Enthalpy ΔH (kJ mol^{-1})	Entropy ΔS (kJ mol^{-1} K^{-1})	ΔG (kJ mol^{-1})			
			293 K	303 K	313 K	323 K
10	-5×10^{-10}	17.559	− 5145.06	− 5320.66	− 5496.26	− 5671.86
20	0	22.165	− 6495.82	− 6717.52	− 6939.22	− 7160.92
30	0	20.301	− 5948.70	− 6151.73	− 6354.76	− 6557.78
40	-1×10^{-9}	20.973	− 6145.45	− 6355.19	− 6564.93	− 6774.68
50	1×10^{-9}	21.783	− 6382.80	− 6600.65	− 6818.49	− 7036.33
60	0	22.132	− 6484.16	− 6705.46	− 6926.76	− 7148.07
70	0	21.666	− 6347.68	− 6564.33	− 6780.97	− 6997.62

evaluated for all the kinetic model predicted results. These metrics are shown in Table 6, for all the four kinetic models. All the statistical values thus resulted are within the acceptable limits and better for non-linear expressions.

To investigate the influence of increase in phenol concentration on the kinetic modelling, the results are presented for only pseudo-first and second-order kinetics for all the concentrations as Table 7. It can be observed that, as the concentration increased, the model fit is getting inferior. From the table, the R^2 values produced from the pseudo-second-order values are higher compared to the pseudo-first order. The increment of the q_e shows that as the concentration of phenol solution increases, the removal of phenol increases. Results show that the capability of the adsorption phenol obeying pseudo-second-order model.

Variation of adsorption capacity against contact time

The adsorption capacity study of removal of phenol is being conducted by using the optimum condition result extracted from the Design-Expert software which is pH value of pH 8, agitation speed of 180 rpm, magnetic biochar dosage of 0.6 g and contact time of 100 min. The concentration of phenol solution is varied from 10 to 70 mg/L, and the maximum contact time for the experiment is 100 min. The phenol samples are being taken at a time interval of 10 min, 30 min, 50 min, 70 min, 90 min and 100 min and being filtered. Then, the absorbance and concentration of the samples are tested using UV-VIS spectrophotometer, and the result of the adsorption capacity is calculated and plotted into a graph which is shown in Fig. 12.

From this graph, it can be observed that the equilibrium state is achieved after 60 min of the reaction time of magnetic biochar and phenol solution. Based on the results, it shows that the equilibrium condition is achieved at 60 min at an increasing amount of concentration of phenol solution. The graph also shows that the higher the concentration of the phenol solution, the higher the values of the adsorption capacity.

Table 9 Review on phenol removal using magnetic biochar

Types of magnetic biochar	q_m (mg/g)	K_L (L/mg)	R^2	k_f (L/g)	n	R^2	Ref
Palm kernel	10.84	0.01	0.983	0.18	1.27	0.996	This study
Rice straw				0.3213	0.9815	0.9867	Li et al. (2017)
Empty fruit bunch	76.31	0.12754	1	9.01	6.9735	0.9998	Mubarak et al. (2016)
Lantana camara (HCl treated)	112.5	0.03951	0.9955	1.3468	5.048	0.9869	Girish and Ramachandra Murty (2014)
Lantana camara (KOH treated)	91.07	0.0386	0.9964	1.326	4.198	0.9811	Girish and Ramachandra Murty (2014)
Eucalyptus seed	0.313	0.796	0.98	1.797	0.442	0.98	Rincón-Silva et al. (2015)
Cyclosorus interruptus	62.6	0.063	0.994	14.2	3.7	0.893	Zhou et al. (2018)
Anaerobic wastewater treatment plant sludge	42.04	0.02	0.969	6.33	3.51	0.9748	Mu'azu et al. (2017)
Wastewater treatment plant sludge	96.154	0.128	0.979	18.065	2.48	0.989	Mu'azu et al. (2017)
Hizikia fusiformis biochar	30.093	49.480	0.961	3.803	1.8939	0.956	Shin (2017)
Iron oxide nano-powder	13.509	0.011	0.992	0.432	1.662	0.982	Mihoc et al. (2014)

Thermodynamic analysis

In the thermodynamic analysis, the study is all about energetic change information that occurs during the adsorption process. The estimated temperatures are used to find the Gibbs free energy (ΔG) value that occurs during the reaction. The other parameters like enthalpy (ΔH) and entropy (ΔS) are calculated based on the following equations (Garba et al. 2016; Rincón-Silva et al. 2015).

$$K = \frac{Ce}{qe}$$

$$\ln K = \left(-\frac{\Delta H°}{RT}\right) + \left(\frac{\Delta S°}{R}\right)$$

$$\Delta G = -RT \ln K$$

Where T is the temperature in unit Kelvin (K), K is equilibrium constant which is equal to Ce/qe, qe is the amount of phenol in aqueous solution adsorbed per unit mass of palm kernel magnetic biochar used, Ce is the equilibrium concentration of phenol in aqueous solution and R is universal gas constant (8.314 J/mol K^{-1}). The calculated values of enthalpy (ΔH), entropy (ΔS) and Gibbs free energy (ΔG) are shown in the table below. Based on the result, the negative values of Gibbs free energy (ΔG) for the adsorption of phenol on the surface of magnetic biochar at different temperatures show that the adsorption process occurs spontaneously and favour toward thermodynamics. Meanwhile, based on the values of entropy (ΔS), it shows that the unpredictability occurs at the solid-solution surface which relates to the increasing number of phenol ions attached to active sides at the magnetic biochar (Gundogdu et al. 2012; Milonjić 2007; Rincón-Silva et al. 2015). The enthalpy values results show that the reaction that occurs in the adsorption process is lowly endothermic and lowly exothermic. Table 8 shows the thermodynamic study for phenol adsorption.

Comparison value of maximum adsorption capacity of phenol using magnetic biochar from previous researches

A study on the comparison of the value of the maximum adsorption capacity of phenol using other types of magnetic biochar is made by referring to the literature. The capability of the palm kernel magnetic biochar for removal of phenol is proven by comparing the maximum adsorption capacity (q_m) with other magnetic biochar, which is shown in detail in Table 9. The highest q_m value using another type of magnetic biochar reported starting from *Lantana camara* (HCl treated) followed by wastewater treatment plant sludge, *Lantana camara* (KOH treated) and then palm kernel magnetic biochar. The difference of q_m values is due to different properties

of magnetic biochar like surface area, porosity, functional group and structure.

Conclusions

The magnetic palm kernel biochar has proven excellent adsorption characteristics for removal of phenol from wastewater. Statistical analysis reveals that the optimum conditions for the highest removal of phenol were recorded to have pH 8, magnetic biochar 0.6 g, contact time 60 min and agitation speed of 180 rpm. Magnetic palm kernel biochar emerge as a better promising adsorbent in the removal of phenol as the removal percentage is more than 93.39.9% with maximum adsorption capacities (qm) of 10.84 mg/g. Both Langmuir and Freundlich isotherm models match the experimental data very well and adsorption kinetic obeyed pseudo-second. Hence, magnetic-based biochar is a potential candidate for wastewater treatment.

References

Abdel-Ghani N, Fouad G, Helal FS (2014) Individual and competitive adsorption of phenol and nickel onto multiwalled carbon nanotubes. J Adv Res 6:405–415

Abdelkreem M (2013) Adsorption of phenol from industrial wastewater using olive mill waste. APCBEE Proc 5:349–357

Abdelwahab O, Amin NK (2013) Adsorption of phenol from aqueous solutions by Luffa cylindrica fibers: kinetics, isotherm and thermodynamic studies. Egypt J Aquat Res 39:215–223

Al Zarooni M, Elshorbagy W (2006) Characterization and assessment of Al Ruwais refinery wastewater. J Hazard Mater 136:398–405

Alam Khan M, Ahmad A (2016) Kinetics and thermodynamic studies of phenol adsorption on nanocomposite. Desalination Water Treat 57: 11255–11265

Alam M, Ameem ES, Muyibi S, Kabbashi N (2009a) The factors affecting the performance of activated carbon prepared from oil palm empty fruit bunches for adsorption of phenol. 155 191–198 pp

Alam MZ, Ameem ES, Muyibi SA, Kabbashi NA (2009b) The factors affecting the performance of activated carbon prepared from oil palm empty fruit bunches for adsorption of phenol. Chem Eng J 155:191–198

Amoatey P, Bani PR (2011) Wastewater management. Waste Water - Evaluation and Management:379–398

Anyika C, Asri NAM, Majid ZA, Yahya A, Jaafar J (2017) Synthesis and characterization of magnetic activated carbon developed from palm kernel shells. Nanotechnol Environ Eng 2:16

Archana V, Meera S, Begum KM, Anantharaman N (2016) Studies on removal of phenol using ionic liquid immobilized polymeric microcapsules. Arab J Chem 9:371–382

Asmaly H, Khan I, Abussaud B, Saleh T, Laoui T, Gupta V, A A (2015) Adsorption of phenol on aluminum oxide impregnated fly ash. 57 6801–6808 pp

Ayotte P, Smith RS, Stevenson KP, Dohnlek Z, Kimmel GA, Kay BD (2001) Effect of porosity on the adsorption, desorption, trapping,

and release of volatile gases by amorphous solid water. J Geophys Res 106:33387–33392

Baig SA, Lou Z, Hayat MT, Fu R, Liu Y, Xu X (2016) Characterization of magnetic biochar amended with silicon dioxide prepared at high temperature calcination. 34:597

Bohdziewicz J, Kamińska G, Tytła M (2012) The removal of phenols from wastewater through sorption on activated carbon. 5:89–94

Chakraborty S, De S, Dasgupta S, Basu J (2005): Adsorption study for the removal of a basic dye: experimental and modeling, 58, 1079–86 pp

Coniglio MS, Busto VD, González PS, Medina MI, Milrad S, Agostini E (2008) Application of Brassica napus hairy root cultures for phenol removal from aqueous solutions. Chemosphere 72:1035–1042

Dahalan F (2014) Phenol and its toxicity, 2, 11–24 pp

Dakhil I (2013) Removal of phenol from industrial wastewater using sawdust, 3, 25–31 pp

Devi P, Saroha AK (2014) Synthesis of the magnetic biochar composites for use as an adsorbent for the removal of pentachlorophenol from the effluent. Bioresour Technol 169:525–531

Dilekoglu M (2016) Use of genetic algorithm optimization technique in the adsorption of phenol on banana and grapefruit peels, 38

Elgarahy AM, Elwakeel KZ, Elshoubaky GA, Mohammad SH (2019) Microwave-accelerated sorption of cationic dyes onto green marine algal biomass. Environ Sci Pollut Res 26:22704–22722

Elwakeel KZ, El-Sayed GO, Abo El-Nassr SM (2015) Removal of ferrous and manganous from water by activated carbon obtained from sugarcane bagasse. Desalin Water Treat 55:471–483

Elwakeel KZ, Aly MH, El-Howety MA, El-Fadaly E, Al-Said A (2018) Synthesis of chitosan@activated carbon beads with abundant amino groups for capture of Cu(II) and Cd(II) from aqueous solutions. J Polym Environ 26:3590–3602

Farhod APDK (2010) Study the adsorption phenomena of phenol from industrial wastewater using commercial powdered activated carbon by using isotherm models, 28, 1186–1195 pp

Gami AA, Shukor MY, Khalil KA, Dahalan FA, Khalid A, Ahmad SA (2014) Phenol and its toxicity: a short review. 1–27

Gao Y, Pramanik A, Begum S, Sweet C, Jones S, Alamgir A, Ray PC (2017) Multifunctional biochar for highly efficient capture, identification, and removal of toxic metals and superbugs from water samples. ACS Omega 2:7730–7738

Garba A, Nasri NS, Basri H, Ismail R, Abdul Majid Z, Hamza UD, Mohammed J (2016) Adsorptive removal of phenol from aqueous solution on a modified palm shell-based carbon: fixed-bed adsorption studies. Desalin Water Treat 57:29488–29499

Gholizadeh A, Kermani M, Gholami M, Farzadkia M, Yaghmaeian K (2013) Removal efficiency, adsorption kinetics and isotherms of phenolic compounds from aqueous solution using rice bran ash, 25, 3871–3878 pp

Girish CR, Ramachandra Murty V (2014) Adsorption of phenol from aqueous solution using Lantana camara, forest waste: kinetics, isotherm, and thermodynamic studies. International Scholarly Research Notices 2014:201626

Gundogdu A, Duran C, Senturk HB, Soylak M, Ozdes D, Serencam H, Imamoglu M (2012) Adsorption of phenol from aqueous solution on a low-cost activated carbon produced from tea industry waste: equilibrium, kinetic, and thermodynamic study. J Chem Eng Data 57: 2733–2743

Gupta AK, Ahmad M (2012) Assessment of cytotoxic and genotoxic potential of refinery waste effluent using plant, animal and bacterial systems. J Hazard Mater 201-202:92–99

Hsieh F-M, Huang C, Lin T-F, Chen Y-M, Lin J-C (2008) Study of sodium tripolyphosphate-crosslinked chitosan beads entrapped with Pseudomonas putida for phenol degradation. Process Biochem 43: 83–92

Inyinbor AA, Adekola FA, Olatunji GA (2016) Kinetics, isotherms and thermodynamic modeling of liquid phase adsorption of rhodamine B dye onto Raphia hookerie fruit epicarp. Water Resources and Industry 15:14–27

Jiboury DKFCA (2013) Adsorption of phenol from industrial wastewater using commercial powdered activated carbon. ICOEST Cappadocia 2013:114–124

Kargari A, Abbassian K (2015) Study of phenol removal from aqueous solutions by a double emulsion (W/O/W) system stabilized with polymer, 50, 150211124006007 pp

Karri RR, Sahu JN (2018) Modeling and optimization by particle swarm embedded neural network for adsorption of zinc (II) by palm kernel shell based activated carbon from aqueous environment. J Environ Manag 206:178–191

Karri RR, Jayakumar NS, Sahu JN (2017a) Modelling of fluidised-bed reactor by differential evolution optimization for phenol removal using coconut shells based activated carbon. J Mol Liq 231:249–262

Karri RR, Sahu JN, Jayakumar NS (2017b) Optimal isotherm parameters for phenol adsorption from aqueous solutions onto coconut shell based activated carbon: error analysis of linear and non-linear methods. J Taiwan Inst Chem Eng 80:472–487

Karri RR, Tanzifi M, Tavakkoli Yaraki M, Sahu JN (2018) Optimization and modeling of methyl orange adsorption onto polyaniline nano-adsorbent through response surface methodology and differential evolution embedded neural network. J Envi Manage 223:517–529

Lee W-H, Tseng T-Y, Hennings D (2001) Effects of ceramic processing parameters on the microstructure and dielectric properties of (Ba1-xCax)(Ti0.99-y′ ZryMn0.01)O3 sintered in a reducing atmosphere. J Mater Sci Mater Electron 12:123–130

Li H, Mahyoub SAA, Liao W, Xia S, Zhao H, Guo M, Ma P (2017) Effect of pyrolysis temperature on characteristics and aromatic contaminants adsorption behavior of magnetic biochar derived from pyrolysis oil distillation residue. Bioresour Technol 223:20–26

Lingamdinne LP, Koduru JR, Chang YY, Karri RR (2018) Process optimization and adsorption modeling of Pb(II) on nickel ferrite-reduced graphene oxide nano-composite. J Mol Liq 250:202–211

Ma H, Li J-B, Liu W-W, Miao M, Cheng B-J, Zhu S-W (2015) Novel synthesis of a versatile magnetic adsorbent derived from corncob for dye removal. Bioresour Technol 190:13–20

Mihoc G, Ianoş R, Păcurariu C (2014) Adsorption of phenol and p-chlorophenol from aqueous solutions by magnetic nanopowder, 69, 385–91 pp

Milonjić SK (2007) A consideration of the correct calculation of thermodynamic parameters of adsorption. J Serb Chem Soc 72:1363–1367

Molva M (2004) Removal of phenol from industrial wastewaters using lignitic coals. 1–90

Mu'azu N, Jarrah N, Zubair M, Alagha O (2017) Removal of phenolic compounds from water using sewage sludge-based activated carbon adsorption: a review. Int J Environ Res Public Health 14:1094

Mubarak NM, Sahu JN, Abdullah EC, Jayakumar NS (2016) Palm oil empty fruit bunch based magnetic biochar composite comparison for synthesis by microwave-assisted and conventional heating. J Anal Appl Pyrol 120:521-528

Owa FD (2013): Water pollution: sources, effects, control and management, 8

Panagos P, Van Liedekerke M, Yigini Y, Montanarella L (2013) Contaminated sites in Europe: review of the current situation based on data collected through a European network, 2013, 158764 pp

Pradeep NV, Anupama S, Navya K, Shalini HN, Idris M, Hampannavar US (2015) Biological removal of phenol from wastewaters: a mini review. Appl Water Sci 5:105–112

Qiu Y, Zheng Z, Zhou Z, Daniel Sheng G (2009) Effectiveness and mechanisms of dye adsorption on a straw-based biochar, 100, 5348–51 pp

Rincón-Silva NG, Moreno-Piraján JC, Giraldo LG (2015) Thermodynamic study of adsorption of phenol, 4-chlorophenol, and 4-nitrophenol on activated carbon obtained from eucalyptus seed. J Chem 2015:12

Rincón-Silva NG, Moreno-Piraján JC, Giraldo L (2016) Equilibrium, kinetics and thermodynamics study of phenols adsorption onto activated carbon obtained from lignocellulosic material (Eucalyptus Globulus labill seed). Adsorption 22:33–48

Ruthiraan M, Abdullah EC, Mubarak NM, Noraini MN (2017) A promising route of magnetic based materials for removal of Cadmium and methylene blue from waste water. J Environ Chem Eng 5:1447–1455

Ruthiraan M, Mubarak NM, Abdullah EC, Mohammad Khalid, Nizamuddin S, Walvekar R, Karri RR (2019) An overview of magnetic material: preparation and adsorption removal of heavy metals from wastewater. Magnetic Nanostructures :131-159. https://doi.org/10.1007/978-3-030-16439-3_8

Said M, Ahmad A, Mohammad A (2013) Removal of phenol during ultrafiltration of palm oil mill effluent (POME): effect of pH, ionic strength, pressure and temperature, 5, 190–196 pp

Shahamat YD, Farzadkia M, Nasseri S, Mahvi AH, Gholami M, Esrafili A (2014) Magnetic heterogeneous catalytic ozonation: a new removal method for phenol in industrial wastewater. J Environ Health Sci Eng 12:50–50

Shin W-s (2017) Adsorption characteristics of phenol and heavy metals on biochar from Hizikia fusiformis. Environ Earth Sci 76:782

Sihem A, LehocineM B, A M (2012) Batch adsorption of phenol from industrial waste water using cereal by-products as a new adsrbent. Energy Procedia 18:1135–1144

Tao K, Dou H, Sun K (2008) Interfacial coprecipitation to prepare magnetite nanoparticles: concentration and temperature dependence. Colloids Surf A Physicochem Eng Asp 320:115–122

Taylor H (2003) Drinking water microbiology, handbook of water and wastewater microbiology. Academic Press, United Kingdom, pp 611–626

Thines KR, Abdullah EC, Mubarak NM, Ruthiraan M (2017a) In-situ polymerization of magnetic biochar–polypyrrole composite: a novel application in supercapacitor. Biomass Bioenergy 98:95–111

Thines KR, Abdullah EC, Mubarak NM, Ruthiraan M (2017b) Synthesis of magnetic biochar from agricultural waste biomass to enhancing route for waste water and polymer application: a review. Renew Sust Energ Rev 67:257–276

Tran HN, You S-J, Hosseini-Bandegharaei A, Chao H-P (2017) Mistakes and inconsistencies regarding adsorption of contaminants from aqueous solutions: a critical review. Water Res 120:88–116

Tziotzios G, Teliou M, Kaltsouni V, Lyberatos G, Vayenas DV (2005) Biological phenol removal using suspended growth and packed bed reactors. Biochem Eng J 26:65–71

Wu M, Ma J, Cai Z, Tian G, Yang S, Wang Y, Xe L (2015) Rational synthesis of zerovalent iron/bamboo charcoal composites with high saturation magnetization. RSC Adv 5:88703–88709

Xin O, Yitong H, Xi C, Chen J (2016) Magnetic biochar combining adsorption and separation recycle for removal of chromium in aqueous solution, 75, wst2016610 pp

Yap MW, Mubarak NM, Sahu JN, Abdullah EC (2017) Microwave induced synthesis of magnetic biochar from agricultural biomass for removal of lead and cadmium from. J Ind Eng Chem 45:287-295

Zhang M, Gao B, Varnoosfaderani S, Hebard A, Yao Y, Inyang M (2013) Preparation and characterization of a novel magnetic biochar for arsenic removal. Bioresour Technol 130:457–462

Zhang X, Rajagopalan K, Lei H, Ruan R, Sharma BK (2017) An overview of a novel concept in biomass pyrolysis: microwave irradiation. Sustain Energy Fuels 1:1664–1699

Zhou X, Zhou J, Liu Y, Wang Y, Ren J, Ling B (2018) Preparation of magnetic biochar derived from cyclosorus interruptus for the removal of phenolic compounds: characterization and mechanism. Sep Sci Technol 53:1307–1318